JOURNAL OF CATALYSIS 72, 199–209 (1981)

Microreactor and Electron Spectroscopy Studies of Fischer–Tropsch Synthesis on Magnetite

H. J. KREBS, H. P. BONZEL, AND W. SCHWARTING

Institut für Grenzflächenforschung und Vakuumphysik, Kernforschungsanlage Jülich GmbH, 5170 Jülich, Federal Republic of Germany

AND

G. GAFNER

National Physical Research Laboratory, CSIR, Pretoria 0001, Republic of South Africa

Received August 11, 1980; revised February 11, 1981

The Fischer–Tropsch synthesis from CO and H_2 (1 : 3 mixture) at 1 bar total pressure and 570 K has been studied in a differential microreactor system on reduced and unreduced Fe_3O_4 (magnetite). The catalytic reactivity data were complemented by surface analytical measurements using Auger electron and X-ray photoelectron spectroscopy (XPS, ESCA). XPS measurements showed evidence of carbon deposition, mostly in the form of graphite on all samples. The rate of methanation on reduced magnetite was characterized by a maximum and subsequent decrease. Both features were dependent on the reduction history of the sample. All samples gave rise to the production of higher-molecular-weight species. The selectivity of reduced magnetite tended towards the formation of saturated hydrocarbons while that of the unreduced magnetite favoured the formation of alkenes. It was concluded that the reduction of magnetite led to a considerable increase in surface area and porosity and that secondary reactions of the alkenes caused the primary product spectrum to shift from alkenes to alkanes. Accordingly the polymerisation probability increased from 0.3 for unreduced magnetite (also for clean foil) to ≥ 0.42 for reduced magnetite.

1. INTRODUCTION

The oxides of iron with various promoting additives, such as Al_2O_3, CuO, and K_2O, represent the basis of many commercial Fischer–Tropsch catalysts. The most commonly used iron oxide is magnetite, Fe_3O_4. Numerous reactivity studies on promoted iron-based catalysts have been published in the literature (1–3). These catalysts are generally reduced in hydrogen prior to their use in synthesis. Several interesting questions exist in this context. How fast and how complete is the reduction of the iron oxide? Is the iron oxide reduced under synthesis conditions? What are the mechanisms of catalyst degradation during synthesis from CO and hydrogen? In an attempt to answer these questions, we have carried out model studies of the reduction of magnetite and of hydrocarbon synthesis from CO and hydrogen on reduced magnetite by using a combination of surface analytical techniques and reaction kinetic data. The surface analysis was performed with Auger electron spectroscopy (AES) and X-ray photoelectron spectroscopy (XPS, ESCA). Reaction kinetics were studied at 1 bar total pressure in a CO/H_2 mixture of 1 : 3. The ability to transfer samples between the catalytic microreactor and the ultrahigh vacuum system in which surface analysis was performed permitted correlation of surface composition and reaction kinetic data.

The results of the present study show

0021-9517/81/120199-11$02.00/0

that magnetite can be reduced at 770 K in 1 bar hydrogen to elemental iron particles. The catalytic activity of these iron particles at 570 K is time dependent. Surface analysis shows the accumulation of largely graphitic carbon on these iron particles. This graphitic carbon seems to be responsible for the decrease in catalytic activity with time. The reduced magnetite thus appears to exhibit behaviour very similar to that of clean polycrystalline iron foils (*4–6*).

2. EXPERIMENTAL

The experimental system consists of a stainless-steel ultrahigh vacuum (UHV) chamber and an attached sample transfer system containing a small microreactor (4 cm^3 volume). The UHV system is equipped with a hemispherical analyzer for AES and XPS (Leybold–Heraeus). This system also possesses provisions for argon sputtering, residual gas analysis, and gas exposures. The sample is in the form of a block of dimensions 6.5 × 6.0 × 1.1 mm cut from a large block of solid magnetite which was made for us at Sasol Ltd. by casting molten magnetite into a magnetite-lined crucible. Sample heating is by direct contact between the magnetite block and a joule-heated molybdenum foil on which it rests. Temperature is measured by a Chromel–Alumel thermocouple attached to the underside of the foil. Other details of this experimental setup have been described elsewhere (*5*).

The sample could be transferred by a valveless air lock system into the catalytic microreactor (Leybold–Heraeus). The mixture of CO/H_2 flowed continuously through this reactor at a rate of 5 cm^3/min. This gas flow and the catalyst volume give a space velocity of 7000 hr^{-1}. The partial-pressure ratio of CO to H_2 was set at 1 : 3 by adjusting the individual flow rates of these gases before they entered the mixing stage. The reaction gases CO and H_2 were 99.999% pure and were passed over chromium oxide absorption cells (Messer–Griesheim "Oxisorb") for further purification. The CO line contained in addition a heated carbonyl trap for the decomposition of Ni carbonyl. The magnetite was reduced at 770 K in 1 bar H_2 flowing at 10 cm^3/min.

The synthesis gas and reaction products were analyzed by gas chromatography (GC, Hewlett–Packard 5834A) using a molecular sieve column and thermal conductivity detector for the synthesis gas and a Poropak Q column and flame ionization detection (FID) for the reaction products. The column temperature was normally 160°C. Other details concerning product detection and reactivity measurements have been specified previously (*5*).

Sputtering of the samples under UHV was carried out by using a plasma discharge sputtering gun (Leybold–Heraeus IQP 10-63) operated with a current density of about 30 $\mu A/cm^2$ and a beamwidth (FWHM) of about 1.0 cm. The ion energy was set at 4.5 keV.

The XPS data were taken with a Mg$K\alpha$ X-ray source generally operated at 10 kV and 300 W power. The pass energy of the spectrometer was set at either 100 or 150 eV. The XPS binding energies were referenced against the graphitic carbon peak at 285.0 eV which was always observed on iron foils and reduced magnetite after a longer reaction time (>30 min) (*5, 6*).

3. RESULTS AND DISCUSSION

We report the results of this investigation in different subsections. In the first section we present surface composition data obtained with Auger and photoemission spectroscopy. The second section deals with the time dependence of the methanation rate of reduced and unreduced magnetite samples. In the third section we present data on the product distribution and its time dependence.

3.1. Surface Composition Data

The freshly prepared magnetite sample was inserted into the UHV system and outgassed at 420 K for about 2 min. AES and XPS spectra were taken at this stage. Fig-

ure 1 shows a summary of Auger spectra. Spectrum (a) represents the initial state of the outgassed magnetite sample. Note the severe carbon and oxygen contamination and the low intensity of the Fe transitions.

The sample was then transferred into the microreactor for a 1-hr reduction at 770 K in flowing H_2 at 1 bar. The reduced sample was transferred back into the UHV system to record its Auger spectrum (b). This showed a substantial decrease in the intensities of the carbon and oxygen transitions and an increase in the iron transitions at 60 and 550–700 eV. The sample was then processed further in UHV by annealing at 1070 K for 2 min and sputtering with argon ions for a total of 20 min. Auger spectrum (c) characterizes the state of the surface following this treatment. Note the large increase in the iron Auger transitions and the small residual amounts of carbon and oxygen. The carbon Auger peak shape at this stage is typical of carbidic (atomic) carbon (*6*). This procedure showed that the contamination of the reduced magnetite sample still visible in spectrum (b) was mainly located at the surface because it could be removed by a simple surface treatment. It is likely that some of this surface contamination occurs during sample transfer from the microreactor to the UHV system.

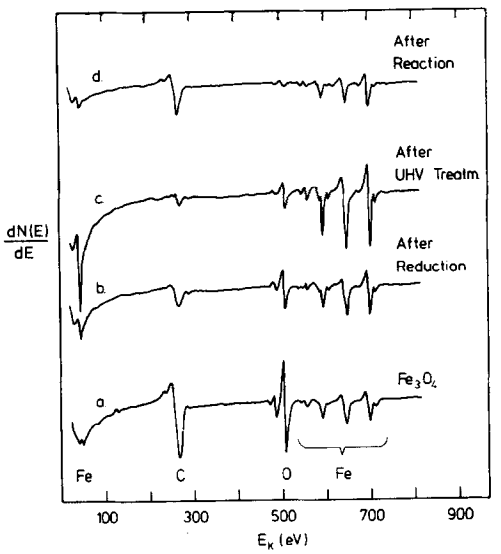

FIG. 1. Auger electron spectra of (a) unreduced magnetite, (b) after 1 hr reduction at 770 K in 1 bar H_2, (c) after additional annealing at 1070 K under UHV for 2 min and 20 min of Ar sputtering, (d) after 3.5 hr reaction at 570 K in $CO/H_2 = 1:3$.

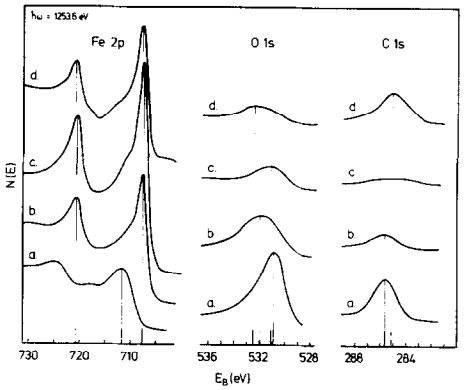

FIG. 2. X-Ray photoelectron spectra of Fe 2*p*, O 1*s*, and C 1*s* peaks; experimental conditions same as in Fig. 1.

The reduced magnetite sample was then moved into the microreactor for hydrocarbon synthesis. The reaction conditions were 570 K and CO/H_2 ratio of 1 : 3. After 2.5 hr of reaction the sample was returned to the UHV system for further surface analysis. Spectrum (d) in Fig. 1 indicates that large amounts of carbon were deposited on the iron sample during the reaction. A small oxygen Auger peak is noted in spectrum (d) which is presumably due to the dissociative adsorption of residual water in the reactor. No oxidation of the sample occurred during the reaction, as will be seen more clearly from the XPS spectra presented below.

The Auger spectra in Fig. 1 illustrate semiquantitatively the surface compositional changes occurring after reduction in H_2 and reaction in a CO/H_2 mixture. More quantitative information is contained in the corresponding XPS data which are summarized in Fig. 2. This figure contains the Fe 2*p*, O 1*s*, and C 1*s* core level spectra recorded for the same conditions as outlined above for Fig. 1. The Fe 2*p* spectra of magnetite, curve (a), closely resemble those given by Brundle *et al.* (*7*). The Fe $2p_{3/2}$ region has a maximum at about 711.8

eV (Fe^{III}) and is broadened on the lower binding energy side (Fe^{II}). After reduction a large shift to a binding energy of 707.8 eV (Fe^0) is noted, with little evidence of any remanent oxidic iron. After removal of surface contamination in UHV (spectrum (c)) the intensities of the Fe $2p$ peaks increase further without any changes in peak positions. The Fe $2p_{1/2}$ peak appears strongly at 720.8 eV.

The O $1s$ peak is originally at 530.9 eV, as seen in spectrum (a), and shifts to 532.0 eV after reduction (spectrum (b)). This supports the viewpoint of Allen *et al.* (*8*) and Haber *et al.* (*9*) who attribute the latter value to the presence of hydroxyl groups which would be expected after reduction. The subsequent UHV treatment, annealing and sputtering, destroys the hydroxyl groups and consequently the O $1s$ peak is again found at around 531.0 eV. Finally, spectrum (d) shows an O $1s$ peak at 532.5 eV which could be due to chemisorbed molecular CO (*6, 7, 10*).

The strong C $1s$ carbon impurity peak which was present after sample preparation at a binding energy of 285.7 eV showed a diminution in height by a factor of about 4 after reduction without any noticeable shift. The UHV surface cleaning treatment which followed removed nearly all carbon, as seen in spectrum (c). Finally, the C $1s$ peak measured after reaction in spectrum (d), has a binding energy of 285.1 eV which is typical for graphitic carbon (*6*). This deposition of graphitic carbon is expected because of the high CO/H_2 ratio of 1:3 (*5*) used in the reaction.

We have also studied the reaction behaviour of an unreduced sample. The XPS data for this experiment are given in Fig. 3. Spectra (a) were taken for the magnetite sample after the initial outgassing procedure under UHV. They are practically identical to those shown in Fig. 2. For some reason the initial carbon contamination seems to be lower than that for the sample in Fig. 2. The sample was then exposed to the 1:3 CO/H_2 mixture at 570 K for a total

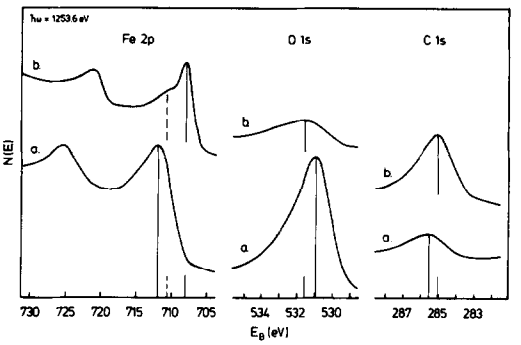

FIG. 3. X-Ray photoelectron spectra of Fe $2p$, O $1s$, and C $1s$ peaks. (a) Unreduced magnetite; (b) after reaction at 570 K in CO/H_2 = 1:3 for 6 hr.

time of 6 hr. The Fe $2p$ spectra in Fig. 3 illustrate that the sample was partially reduced during the reaction because the Fe $2p_{3/2}$ peak is composed of two contributions, a peak at 708.0 eV (Fe^0) and a shoulder at 710.8 eV (Fe^{II}). This peak shape seems to imply that the sample consists of a mixture of reduced Fe and wüstite (FeO).

The O $1s$ spectrum after reaction indicates a small amount of oxygen on the surface. This result is unexpected as the magnetite is only partially reduced. However, the C $1s$ spectrum shows a large amount of contaminating carbon with a binding energy of 285.1 eV. The reaction has thus caused substantial graphite deposition which presumably covers the mixed iron/wüstite surface and hence attenuates the true O $1s$ electron emission. We see from a comparison of Figs. 2 and 3 that the reduction of magnetite is slower in CO/H_2 at 570 K than in pure H_2 at 770 K.

A third kind of sample preparation was carried out under UHV. Here the sample was heat treated and sputtered with argon ions for 30 min. The resulting Fe $2p$ spectra are shown in Fig. 4. Spectrum (a) represents the outgassed magnetite sample. Spectrum (b) was recorded after the UHV processing. Note the shift of the Fe $2p_{3/2}$ peak to the binding energy of 710.8 eV which is characteristic of Fe^{II} (*7*). The combined heating and sputtering of magnetite thus causes a partial reduction of the sur-

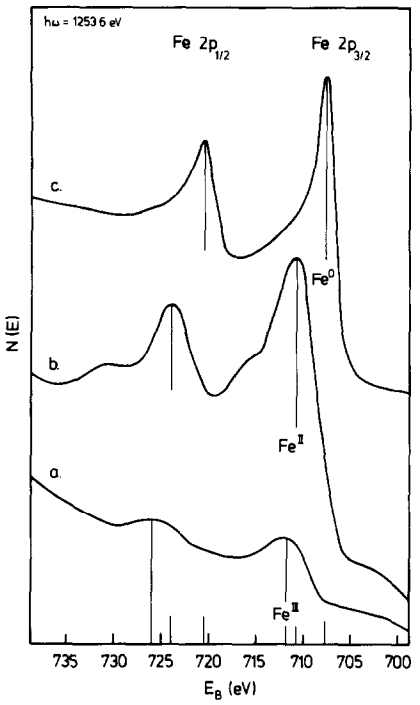

FIG. 4. X-Ray photoelectron spectra of Fe 2*p*. (a) Unreduced magnetite; (b) after Ar sputtering (4.5 keV) for 30 min at ≅ 1000 K and 1 min annealing to 1120 K; (c) for comparison: a sample that was reduced at 770 K in H_2 for 3 min.

face layer to wüstite (FeO). Spectrum (c) in Fig. 4 which was obtained for a magnetite sample reduced in hydrogen for 3 min at 770 K is also included for comparison. A short (3 min) reduction seems to be quite sufficient to change magnetite into fully reduced iron in a layer of at least the thickness of the probing depth of XPS.

3.2. Time Dependence of Methanation

In this section we present reactivity data for magnetite samples in the form of methanation rate versus reaction time curves for reaction at 570 K and a CO/H_2 ratio of 1 : 3. Figure 5 gives results for various magnetite samples which have been reduced in H_2 for different periods of time. For example, the unreduced magnetite sample shows an initially increasing reactivity until a plateau is reached after 80 min. In contrast, a sample reduced in H_2 for 1 min shows a much higher initial reactivity (factor 100) which then decreases rapidly with increasing reaction time until a shallow minimum is reached after 60 min. At this point the reactivity is lower than that of the unreduced magnetite sample. If the reduction time is increased to 3 min, analogous behaviour in reactivity versus time is observed except that the minimum is reached after about 160 min. The reactivity is then comparable with that of the unreduced sample. An increase in the reduction time to 60 min leads to a still higher maximum rate of methanation and a slower subsequent decrease with time. Even after 200 min of reaction the rate is still at least five times larger than that of the unreduced sample. A further increase in the reduction time leads to a decrease in the maximum methanation rate. This behaviour is also illustrated in Fig. 5 by the time-dependent methane generation by a magnetite sample which had been re-

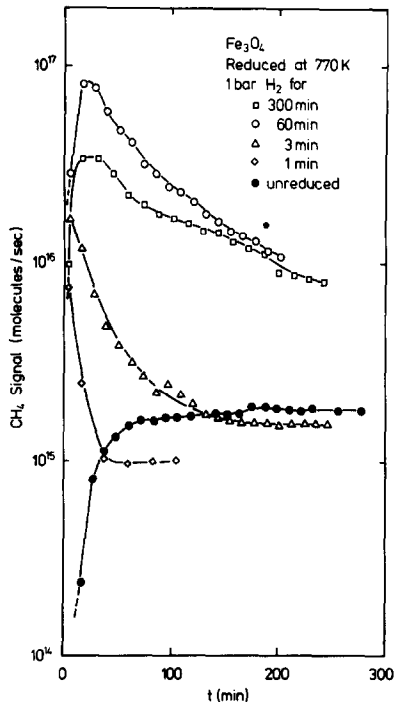

FIG. 5. Initial time dependence of methane formation from CO/H_2 = 1 : 3 at 570 K for magnetite samples which had been reduced prior to reaction for various lengths of time.

duced for 300 min. The maximum is significantly lower than that for the 60-min sample although the rate of decrease is a little smaller giving roughly equal rates after 200 min. Figure 6 summarizes these findings in a plot of maximum methanation rate versus reduction time of magnetite (all at 770 K). The optimum time is between 60 and 100 min.

The dependence of the maximum methanation rate on reduction time, Figs. 5 and 6, can be understood by referring to, on the one hand, an increase in specific surface area during reduction, and on the other hand, the reverse of this process, namely, sintering of iron particles at the reduction temperature. It is well known from the literature (*11*, *12*) that the reduction of magnetite causes a substantial increase in specific surface area and porosity. This trend was confirmed in the present study by scanning electron microscopy of magnetite samples before and after reduction. Figures 7a and b show representative examples of identical surface regions before and after reduction in H_2 (1 hr at 770 K). It can be clearly seen that the reduction causes a significant widening of crevices and opening of pores which is indicative of an increase in surface area. We assume therefore that the total volume and surface area of reduced magnetite increase with increasing reduction time. The time-dependent reactivity data in Fig. 5 then indicate the state of reduction of the total magnetite sample. The larger the volume of reduced magnetite is, the higher the initial rate of methanation is and the slower its rate of decrease. The increase in the amount of reduced material is not visible in the corresponding XPS spectra of iron because of the small probing depth of XPS. The reactivity versus time data in Fig. 5 are therefore a valuable complement to the surface composition XPS data for judging the efficiency of magnetite reduction.

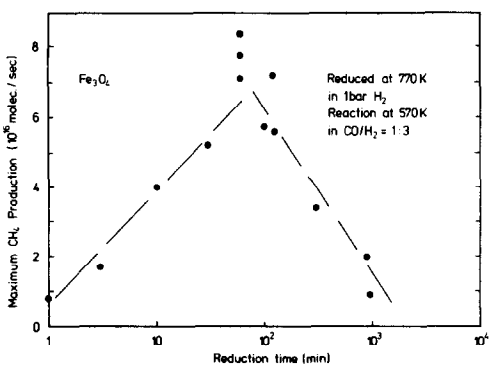

FIG. 6. Maximum rate of methanation as a function of reduction time (for constant size of catalytic sample).

On the other hand, the reduction temperature of 770 K is presumably high enough for some sintering to occur. When the two processes, reduction of magnetite and sintering of reduced iron, are occurring simultaneously the resulting surface area will depend on their relative rates at 770 K. However, regardless of these two rates, the process of sintering will always lead to a decrease in surface area for a totally reduced magnetite sample. It is for this reason that a maximum in the methanation rate with reduction time in Fig. 6 is observed. A lowering of the reduction temperature will decrease the rate of sintering and favour the creation of a larger surface area. This was in fact proven for a reduction at 670 K which gave rise to a higher maximum rate of methanation, in support of the sintering hypothesis.

For comparison, we have also studied the reactivity behaviour of iron foils in reduced and heavily oxidized states. Three different modes of sample preparation and hence initial conditions were used: (A) new polycrystalline Fe foil cleaned under UHV; (B) heavily oxidized Fe foil after heating in air to 1000 K for 5 min; (C) foil oxidized as in (B) and subsequently reduced in H_2 at 670–770 K for 1–15 min. The clean Fe foil A showed a relatively low activity, in accordance with previous observations (*4*, *5*). The oxidized foil B, on the other hand, was characterized by XPS data identical to those for magnetite and showed a reactivity versus time behaviour which was very simi-

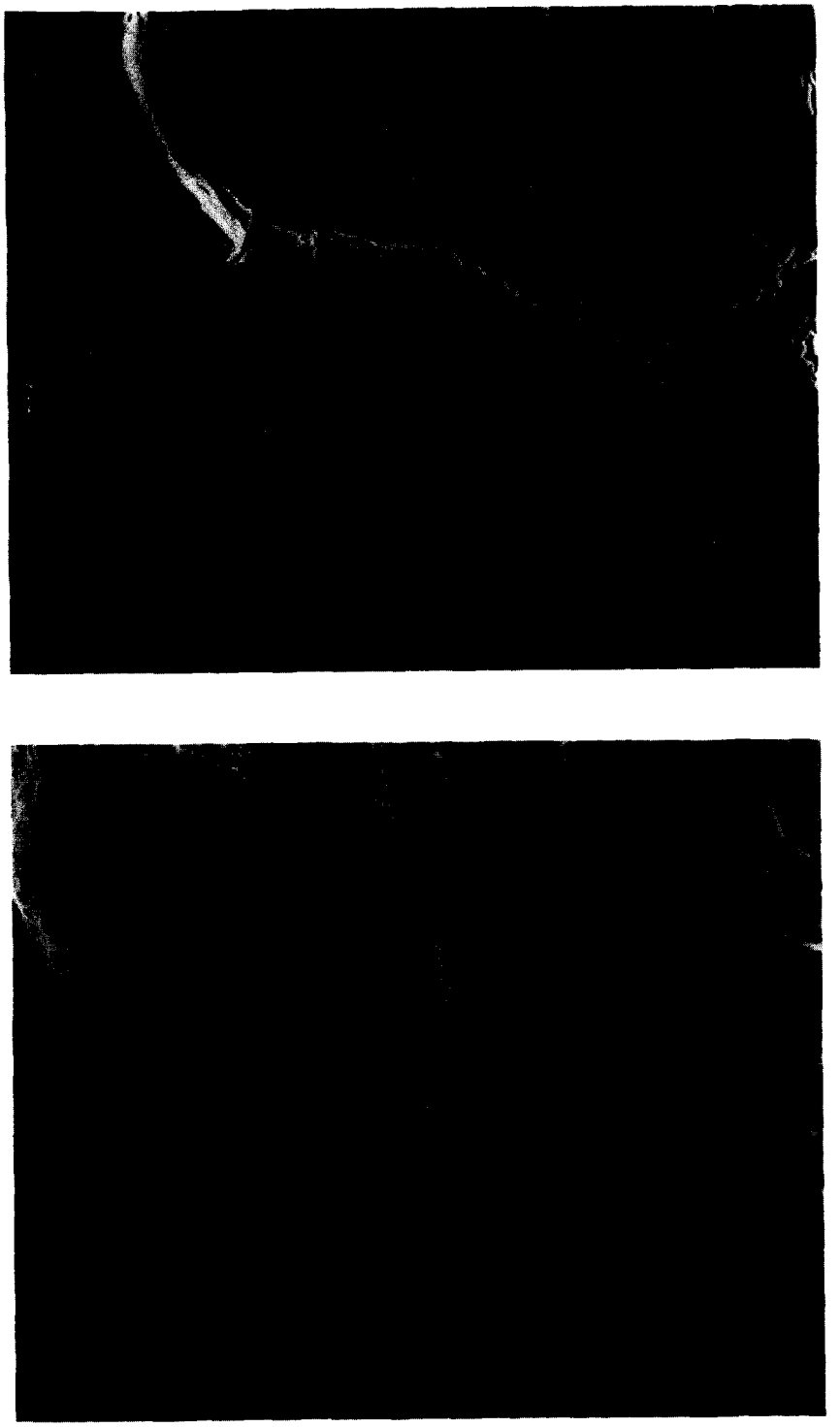

FIG. 7. Scanning electron micrographs of unreduced (upper) and reduced (lower) magnetite; the reduction conditions were 770 K in 1 bar H_2 for 1 hr. Magnification is about 500×. The photographs show the same area of the same sample.

lar to that for unreduced magnetite (Fig. 5). The reactivity was at all times higher than that for clean Fe foil (*4*). However, this reactivity was exceeded by that of the reduced foil C which showed a maximum in the rate of methanation versus time as noted in Fig. 5 for the reduced magnetite samples. It is clear that the same argument as before, namely, a substantial increase in surface area, can be invoked to explain this increase in the methanation rate of the reduced/oxidized foils compared to the oxidized or clean Fe foil.

As seen from the data in Fig. 4, heating and argon sputtering of the unreduced magnetite caused a partial reduction of magnetite to Fe^{II} in a surface region. This partially reduced magnetite, as characterized by spectrum (b) in Fig. 4, was also subjected to the CO/H_2 mixture. The result is given in Fig. 8 as the rate of methanation versus time. These data are very similar to those obtained with the unreduced magnetite sample shown in Fig. 5. The initial increase in reactivity versus time and the plateau reached after about 60 min are only marginally higher than those for the unreduced magnetite. The data for the 3-min reduced magnetite sample are included in Fig. 8 for comparison. The similarity between the unreduced and the UHV-treated samples suggests that the degree of reduction caused by sputtering of magnetite under UHV is insufficient to have a significant effect on the methanation rate.

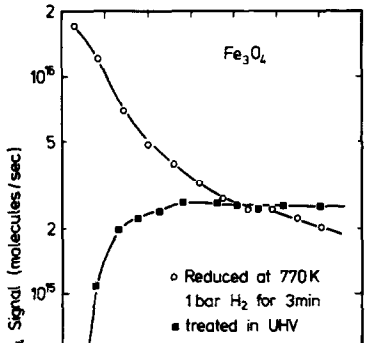

FIG. 8. Initial time dependence of methane formation from CO/H_2 = 1:3 at 570 K for a magnetite sample reduced in H_2 for 3 min, and a sample which was Ar sputtered under UHV (compare Fig. 4 for corresponding Fe 2*p* spectra and experimental conditions).

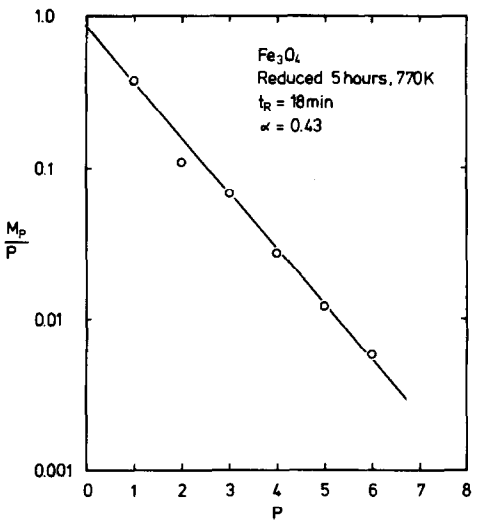

FIG. 9. Schulz–Flory plot (M_P = weight percentage, P = carbon number) of hydrocarbon products after 18 min of reaction at 570 K in CO/H_2 = 1:3; the magnetite sample had been reduced for 5 hr at 770 K in 1 bar H_2.

3.3. Selectivity

All magnetite samples, in their unreduced state as well as after various times of reduction in H_2, produced methane and copious higher-molecular-weight hydrocarbons from a CO/H_2 mixture. A Schulz–Flory plot for a sample which had been reduced at 770 K for 5 hr is presented in Fig. 9. The reaction conditions were the usual 570 K, CO/H_2 = 1:3, 1 bar and the reaction time in this case was 18 min, i.e., close to the maximum activity for methane formation. The polymerisation probability derived from the slope of this plot is α = 0.43. Note the typically low value for C_2 (undershoot) which is always observed when α values are high (*13*).

The time dependence of the identified products for a freshly reduced (1 hr) magnetite sample is shown in Fig. 10 for the

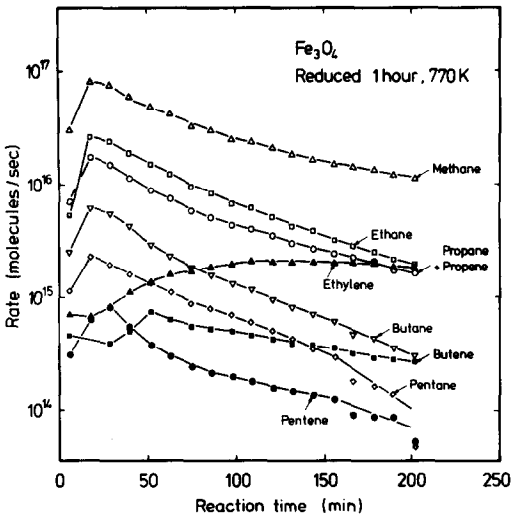

FIG. 10. Time dependence of the product distribution over the first 3.4 hr of reaction in $CO/H_2 = 1:3$ at 570 K. The magnetite sample had initially been reduced for 1 hr at 770 K. Note the different behaviour of alkanes and alkenes.

first ~3 hr. Two important features can be observed. Firstly, the time dependence of all alkanes is similar to that of methane (Fig. 5), and secondly, the time dependence of low-molecular-weight alkenes, in particular ethylene, is significantly different from that of methane. Unfortunately, propylene and propane could not be separated under the present experimental conditions. However, note that the amount of ethylene actually increases with time while butene shows a much lower rate of decrease than butane, and similarly for pentene. The maxima in the rates of formation of the alkenes shift to larger reaction times with decreasing carbon number. These peak times are not highly reproducible but are in the vicinity of 180, 60, and 30 min for ethylene, butene, and pentene, respectively. At the same time the carbon surface concentration increases (*5, 6*). The long-term product spectrum, after about 10 hr, contains essentially only methane and alkenes, and agrees with the result of Pichler *et al.* at high space velocity (*14, 16*).

The data of Fig. 10 were also used to construct Schulz–Flory plots at three different reaction times, viz., 6, 52, and 202 min. These plots are shown in Fig. 11 and illustrate that the chain growth probability α decreases from 0.46 at 6 min to 0.39 at 202 min. One can also see here that the amount of C_2 undershoot becomes less with increasing reaction time and decreasing α. This means that, since the behaviour of ethane is quite normal, ethylene is playing a special role in the chain growing process as has already been proposed (*13*). The total conversion, on a C-atom basis, was calculated from the product spectrum and changes from about 14 to 21 to 4% (with a maximum of 36% at 18 min reaction time) such that the reactor does not operate truly differentially at all times. On the other hand, the total conversion exhibits a maximum just as all products do (Fig. 10), but the chain growth probability shows a monotonic decrease with increasing time. At the same time it is observed that the amount of deposited carbon increases, for reduced magnetite as well as for clean iron foils (*6*). It thus appears that the "clean" Fe surface, i. e., the initial state of the completely reduced magnetite, has the highest chain growing capability as evidenced by the largest α value. This surface is not "clean"

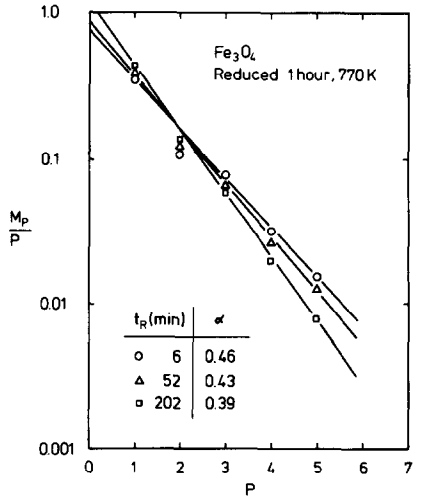

FIG. 11. Schulz–Flory plot of product distribution from Fig. 10 for three reaction times t_R. Note the decrease in α with increasing time.

from a surface physics point of view but most probably covered with a CH_x-type layer which contains a high concentration of chain growing groups (*6*).

It is also interesting to compare the product distribution and α values of reduced and unreduced magnetite. We have seen in Fig. 5 that the time dependence of the reactivities (methane) are quite different and consequently we expect differences in product distributions. Figure 12 compares results for the unreduced magnetite (upper panel) and a magnetite sample which was reduced at 770 K for 1 hr (bottom panel). Approximately equal reaction times were chosen for this comparison. We note that α is considerably smaller for the unreduced sample (here also α decreases with increasing time) and that the percentage of unsaturated products is consequently high. The reduced sample (high α), on the other hand, shows a very low ethylene yield and low percentages of the higher-molecular-weight alkenes. The chain growth probability on reduced magnetite is thus higher than on magnetite. Unfortunately, this comparison is somewhat confused by the increase in specific surface area for the reduced magnetite. Due to the larger surface area *and* porosity it is possible that the diffusion of products out of this catalyst is slower than in the case of unreduced magnetite such that readsorption of products could become more important and influence the product distribution (*13, 15*). For this reason reaction experiments were performed on flat polycrystalline Fe foils in order to limit the possibility of product readsorption while still having totally reduced iron. These experiments, carried out under identical conditions, yielded initial α values of about 0.30 identical to the value for unreduced magnetite. This agreement in α values suggests that Fe_3O_4 becomes superficially reduced at the very beginning of the reaction and that the reaction then takes place on this thin layer of Fe^0. The high value of $\alpha \geqq 0.42$ for reduced magnetite is probably due to reactions of readsorbed primary products, such as, e.g., ethylene. For this reason the relative concentration of ethylene is particularly low in this case.

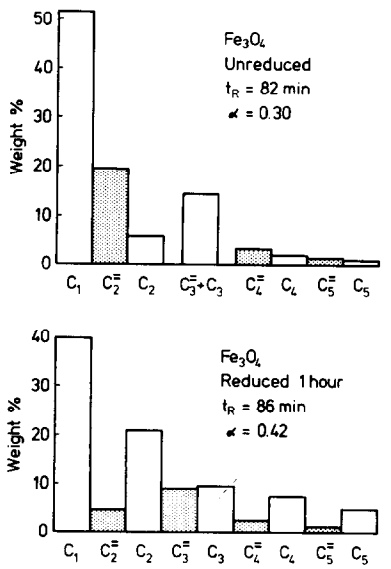

FIG. 12. Comparison of product distributions (wt%) of unreduced and reduced (1 hr at 770 K in H_2) magnetite for about equal reaction times. Reaction conditions were $CO/H_2 = 1:3$ and 570 K. Note the high value of α and the predominance of saturated hydrocarbons in the case of the reduced magnetite sample.

4. CONCLUSIONS

1. The reduction of magnetite at 770 K in H_2 under the present flow conditions leads to an agglomerate of zero-valent iron with a concomitant increase in surface area.

2. The time dependence of methanation from CO/H_2 (1:3) at 570 K complements XPS surface analysis as it allows the progress of magnetite reduction into the bulk of the sample to be monitored.

3. Some sintering of the reduced iron takes place at 770 K in H_2 as evidenced by a lower methanation activity at large reduction times.

4. The reactivity of completely reduced magnetite is analogous to that of clean iron; excessive carbon deposition and graphite formation lead to a decrease in methanation activity with time.

5. The product selectivity of unreduced magnetite is characterized by a large percentage of alkenes and is thus similar to that of clean iron.

6. The selectivity of reduced magnetite shows a high percentage of saturated hydrocarbons and a high polymerisation probability α, both of which are due to secondary reactions of alkenes.

7. The readsorption of primary products is more important on reduced than on unreduced magnetite because of the higher surface area (porosity) of the former.

8. The present study illustrates the usefulness of a combined catalytic microreactor and XPS surface analytical facility featuring a fast and convenient sample transfer system.

ACKNOWLEDGMENTS

We would like to thank Mr. Udo Linke for the SEM investigation of some magnetite samples. One of us (G.G.) wishes to acknowledge the research sponsorship by Sasol Ltd. Dr. M. E. Dry of Sasol Ltd. is thanked for providing the magnetite samples. We are also grateful to George Comsa for critically reviewing this manuscript.

REFERENCES

1. Anderson, R. B., *in* "Catalysis" (P. H. Emmett, Ed.), Vol. 4, p. 119. Reinhold, New York, 1956.
2. Dry, M. E., Shingles, T., and Boshoff, L. J., *J. Catal.* **25,** 99 (1972).
3. Matsumoto, H., and Bennett, C. O., *J. Catal.* **53,** 331 (1978).
4. Dwyer, D. J., and Somorjai, G. A., *J. Catal.* **52,** 291 (1978)
5. Krebs, H. J., Bonzel, H. P., and Gafner, G., *Surf. Sci.* **88,** 269 (1979).
6. Bonzel, H. P., and Krebs, H. J., *Surf. Sci.* **91,** 499 (1980).
7. Brundle, C. R., Chuang, T. J., and Wandelt, K., *Surf. Sci.* **68,** 459 (1977).
8. Allen, G. C., Curtis, M. T., Hooper, A. J., and Tucker, P. M., *J. Chem. Soc. Dalton Trans.*, 1525 (1974).
9. Haber, J., Stoch, J., and Ungier, L., *J. Electron Spectrosc.* **9,** 459 (1976).
10. Kishi, K., and Roberts, M. W., *J. Chem. Soc. Faraday Trans. I* **71** 1751 (1975).
11. Anderson, R. B., *in* "Catalysis" (P. H. Emmett, Ed.), Vol. 4, p. 165. Reinhold, New York, 1956.
12. Hall, W. K., Tarn, W. H., and Anderson, R. B., *J. Amer. Chem. Soc.* **72,** 5436 (1950).
13. Pichler, H., and Schulz, H., *Chem. Ing. Tech.* **42,** 1162 (1970).
14. Pichler, H., Schulz, H., and Hojabri, F., *Brennst. Chem.* **45,** 215 (1964).
15. Dwyer, D. J., and Somorjai, G. A., *J. Catal.* **56,** 249 (1979).
16. Reymond, J. P., Mériaudeau, P., Pommier, B., and Bennett, C. O., *Amer. Chem. Soc. Div. Fuel Chem. Prepr.* **25**(2), 71 (1980).